Tanzania Journal of Science

Volume 51(3), 2025

journal homepage: https://commons.udsm.ac.tz/tjs/

Energy-saving simple adaptive recursive terminal sliding mode control for industrial feed drive systems

Haryson Johanes Nyobuya[Ŧ]

Department of Mechanical and Industrial Engineering, University of Dar es Salaam, Tanzania Email: harysonnyobuya@gmail.com, haryson@udsm.ac.tz

Keywords

Feed drive systems; finite-time; nonlinear control; disturbance rejection; terminal sliding mode control.

Abstract

This paper proposes a simple adaptive recursive terminal sliding mode control approach for industrial feed drive systems. The design employs a recursive sliding mode structure that eliminates the reaching phase and ensures finite-time convergence of the tracking error. To mitigate chattering, a second-order nonsingular terminal sliding mode is used and the parameters to compensate for disturbances are obtain in terms of integral form and a proportional terminal term, which enhances disturbance rejection and further guarantees finite-time convergence. The proposed controller significantly reduces the tracking error and saves energy for the feed drive system. Numerical simulations on an industrial feed drive system confirm the controller's superior performance in terms of fast convergence, contour error reduction, and lower energy usage, especially when compared to a configuration lacking the proportional terminal term. The impact of this work lies in providing a robust and energy-efficient control approach that enhances both precision and energy performance in modern industrial motion systems under disturbances.

Introduction

In the modern manufacturing and production, feed drive systems are among the vital components owing in moving worktables or tools with precision, speed and force for different purposes (Altintas et al. 2011, Halinga et al. 2023, Msukwa and Santos 2021, Nshama et al. 2021, Nyobuya and Uchiyama 2024). Due to tighter tolerances and higher accuracy, the need for accurate motion control becomes even more significant. However, tracking performance not only contributes to product quality but also leads has an impact on the energy usage. Furthermore, since feed drive systems often operate continuously around the clock, they tend to consume a significant amount of energy. Hence, it's vital to propose such ways on which the low energy consumption and high tracking accuracy can be obtained. The most common approach used in the industries for feed drive systems is the Proportional-Derivative controller with knowledge of the dynamics and error dynamics an approach is developed to control the feed drives. However, PD controller is limited, as elaborated in (Zhang and Mohammadzadeh 2025, Msukwa et al. 2020), the overall control performance of the systems tends to depend on the oscillations, external disturbances, and un-modeled uncertainties.

In recent years, control approaches which

[Ŧ]Corresponding author: harysonnyobuya@gmail.com, haryson@udsm.ac.tz

Received 15 Jun 2025; Revised 15 Sept; Accepted 22 October 2025; Published 30 October 2025
https://doi.org/10.65085/2507-7961.1050

ISSN 0856-1761, e-ISSN 2507-7961

are non-linear are proposed to meet the high accuracy and low energy consumption, such approaches including model predictive control by Leipe et al. (2023), model-reference adaptive control by Gai et al. (2021), robust control by Xu et al. (2024), and sliding mode control by Wei et al. (2025) have been applied to control the industrial feed drives at different aspects and achieve high-performance.

It's worth mentioning there are other intelligent techniques also used to control the feed drives systems including Fuzzy control by Yu et al. (2023) and Neural Network-Based control by Zamfirache et al. (2023). Overall, these techniques can produce relative high control performance but their architectures, processes and computation effort make them unfeasible for real-life applications.

Sliding mode control (SMC) is one of the among the non-linear control approach, offers robustness and disturbance rejection this enables high tracking performances to the feed drive system to be improved. The primary advantage for SMC lies in its ability to be insensitive to un-modeled uncertainties and external disturbances, maintain the designed sliding surface state at all times including from the initial state (Gambhire et al. 2021). Sliding mode structure have two parts which are the equivalent control and discontinuous control, the equivalent control ensures that dynamics stay in the sliding surface and the discontinuous part forces the trajectories to the sliding surface upon existence of disturbances and other un-modeled dynamics. SMC is of linear nature for which upon control application it only converges asymptotic and cannot attain finite-time convergence. To attain finite-time convergence, Wu et al. (1998) propose terminal sliding mode (TSM) which modifies the sliding surface with nonlinear terms which forces all the trajectories to the sliding surface to converge to equilibrium in finite-time.

Due to singularity problems of TSM structure, Feng et al. (2002) proposed a non-singular TSM control for which the control architecture attains finite-time without singularity problems. As the result of this advancement, the following researches were inspired, including continuous adaptive fast terminal sliding mode-based speed regulation control proposed by Chen et al. (2023), a fuzzy adaptive PID with fast terminal sliding mode controller proposed by Zhong et al. (2021) for a redundant variable load. Continuous approximation helps eliminate chattering, while fuzzy logic estimates system error and disturbance bounds. The modifications on these designs make the sliding surface design that accelerate the system's response and good performance is obtained.

For continuity and the elimination of chattering, continuous non-singular TSM control is proposed by Yu et al. (2005). Chiu (2012) proposed the integral terminal sliding mode for systems with a relative degree of one, effectively removing the reaching phase to the nonlinear sliding surface and guaranteeing finite-time convergence of both tracking and integral errors.

In practice, disturbances play a significant role on disrupting the accuracy and increase energy consumption while operating the feed drive system. Therefore, it is inevitable to design a controller which is can deal with the disturbances effectively. The primary objective of this paper is to improve the tracking performance by explicitly considering the external disturbances. However, the discontinuous or switching operation is governed by sign function which forces the control architecture into chattering mode. This drawback may cause a relentless damage to the mechanical structure or unstable.

Different ways exist to deal with this problem, including the boundary layer approach (Razzaghian et al. 2022, Dong et al. 2021) where the continuous approximation of signum function is performed by introducing a small boundary for which replaces the signum function with saturation more details are explained by Saha et al. (2021). However, the boundary layer approach is that the sliding mode loses the robustness against uncertainties when the sliding surface reaches inside the boundary layer (Slotine and Li

1991, Boiko 2013).

Another approach for reducing chattering in the control architecture is by using a disturbance observer with sliding mode control. By predicting the designed model uncertainties, the controller compensates the uncertainties without relying on strong switching signals (Önen 2023, Zuo et al. 2023). However, this method acquires an unrealistic magnitude of control input to estimate the disturbance. In addition, the disturbance observer in the system increases the order of the system and, thus, increases the computational complexity (Vo and Kang 2019).

Higher-order SMC (HOSMC) (Utkin 2015, Shtessel et al. 2023, Oliveira et al. 2022) is known approach that alleviates the chattering to a great extent without compromising with the precision of the controlled system performance. The high frequency component of discontinuous control is applied into higher order derivative of sliding surface.

In addition, the chattering component in the actual control input gets attenuated substantially. As a result, the high frequency input cannot be propagated into the sliding surface of the system. More forms of HOSMC approaches have been explored including (Sun et al. 2022, Deng et al. 2020), and references therein.

Deng et al. (2020) proposed an adaptive recursive terminal second-order SMC is proposed for which the reaching phase is eliminated and the finite-time convergence of the tracking error to zero is ensured as compared to ISMC. Furthermore, second order non-singular terminal sliding mode is used for which the reaching control input is achieved in an integral form of the signum function which can effectively suppress chattering.

In this paper, motivated by the principles of high-order sliding mode (HOSM) control, a simple adaptive recursive terminal sliding mode control method is proposed for the industrial feed drive system.

First, the dynamic model of the feed drive system with un-modeled uncertainties and external disturbance is presented. Second, based on the concept of non-singular TSM control and ITSMC, the controller is constructed based on a recursive nature. Moreover, the adaptive parameters in the switching or discontinuous control are designed on terms of integral term which is typically used and proportional terminal term with is proposed. The integral term contributes negative feedback that prevents error growth in the Lyapunov framework, thereby guaranteeing overall system stability. Furthermore, by feeding the integrated error back into the control input, the controller ensures that even small but persistent deviations are driven to zero. The proportional terminal term further suppresses the tracking error and reduces the finite-time convergence with Lyapunov stability guarantee.

This concept is based on simple adaptive control theory explained by Kaufman et al. (2012) for which the adaptation is achieved and in turn reduces the tracking errors and lower the energy consumption.

The remaining paper is organized as follows: the next section presents the feed drive dynamics along with the energy consumption model, followed by the controller design and stability analysis. The subsequent section after, presents the numerical simulation and results, followed by discussion of the results. Finally, the paper concludes with final remarks of the findings.

Table 1: The list of symbols and notations used in this paper

Symbol	Description
i	Index of the axis $(i=1,2)$
q_i	Position of the feed drive axis
q_{di}	Reference position of the axis
e_i	Tracking error

m_i	Mass parameter of the axis
m_{0i}	Nominal (estimated) mass
Δm_i	Mass uncertainty
c_i	Viscous friction coefficient
c_{0i}	Nominal viscous friction coefficient
Δc_i	Uncertainty in viscous friction
L_i	Coulomb friction force
L_{0i}	Nominal Coulomb friction
ΔL_i	Uncertainty in Coulomb friction
d_i	External disturbance
τ_i	Control input torque/force applied to axis
ρ_i	Lumped uncertainty and disturbance term
a_{ji}	Unknown positive constants bounding $\dot{\rho}_i$, $j=0,1,2,3$
σ_i	Non-singular terminal sliding surface
$\lambda_{1i}, \lambda_{2i}$	Positive control gains in terminal sliding surface
γ_{1i}, γ_{2i}	Nonlinear exponents in terminal sliding surface
$sig(x)^y = \lvert x \rvert^y s$	Signum power function
s_i	Recursive integral terminal sliding surface
σ_{iI}	Integral sliding variable
v_{1i}, v_{2i}	Positive odd integers for integral sliding dynamics
τ_{eqi}	Equivalent control input
τ_{swi}	Switching (discontinuous) control input
$\hat{a}_{ji}$	Estimated adaptive gains, $j=0,1,2,3$
$\hat{a}_{jIi}$	Integral adaptive gains
$\hat{a}_{jpi}$	Proportional adaptive gains
η_{jIi}, η_{jpi}	Positive adaptation rate constants
$\beta_i=\beta_{1i}/\beta_{2i}$	Ratio of odd integers for proportional adaptive law
V_i	Lyapunov candidate function
μ_{ji}	Positive weighting constants in Lyapunov function
$\tilde{a}_{ji}$	Estimation error for adaptive parameters
σ_{si}	Lumped disturbance margin term
σ_{ji}	Terms associated with adaptive error stability
σ_{pi}	Positive term for proportional adaptive convergence
Γ_{1i}, Γ_{2i}	Positive constants ensuring finite-time stability
t_{vi}, t_{si}, t_{ci}	Convergence times for Lyapunov function, sliding variable, and tracking error respectively

Feed Drive System Dynamics

The dynamics of the feed drive systems are of many configurations, a typical biaxial setup, also referred to as X-Y table with 2 axes, is considered in this paper represented as format as follows:

$$m_i \ddot{q}_i + c_i \dot{q}_i + L_i sgn(\dot{q}_i) + d_i = \tau_i, i(1,2) \quad (1)$$

whereas m_i, c_i, and L_i corresponds to the mass, viscous friction coefficient, and Coulomb friction force for each individual drive axis i. The control input applied to each axis is denoted by τ_i, while d_i, and q_i are the external disturbance and position of each drive axis. Given that the drive axes are actuated by servo motors mechanically coupled to the system, their dynamic characteristics are included in the system formulation. It is assumed that feed drive system posses the following uncertainties:

$$m_i = m_{0i} + \Delta m_i, c_i = c_{0i} + \Delta c_i, L_i = L_{0i} + \Delta L_i, \quad (2)$$

where m_{0i}, c_{0i}, and L_{0i} are estimated terms and Δm_i, Δc_i, and ΔL_i are uncertainty terms. Then, the dynamic equation of the feed drive system can be written as

$$m_{0i} \ddot{q}_i + c_{0i} \dot{q}_i + L_{0i} sgn(\dot{q}_i) = \tau_i + \rho_i \quad (3)$$

with

$$\rho_i = -\Delta m_i \ddot{q}_i - \Delta c_i \dot{q}_i - \Delta L_i - d_i \quad (4)$$

From (3)-(4), it's obvious that ρ_i is linearly affected by q_i,$\dot{q}_i$, and $\ddot{q}_i$. The derivative of ρ_i can reasonably be assumed to be bounded by

$$\frac{1}{m_{0i}} |\dot{\rho}_i| < a_{0i} + a_{1i} |q_i| + a_{2i} |\dot{q}_i| + a_{3i} |\ddot{q}_i|, \quad (5)$$

where a_{ji}, $(j=0,1,2,3)$ are positive numbers that tend to exists but unknown. Such bounds are commonly employed in control theory to ensure system stability or to design robust controllers when exact parameter values are unknown but assumed to exist such as (Deng et al. 2020).

Control Design

The control objective is to design a controller to achieve precise, energy-saving and fast tracking performance of the feed drive system in the existence of system uncertainties. The positional tracking error of the system as follows:

$$e_i = q_{di} - q_i, \quad (6)$$

where $q_{di}$is the reference position. From (3), the error dynamics can be written as

$$\ddot{e}_i = \ddot{q}_{di} - \frac{1}{m_{0i}} \{\tau_i - c_{0i} \dot{q}_i - L_{0i} sgn(\dot{q}_i) - \rho_i\}, \quad (7)$$

The objective for the feed-drive system to follow the reference trajectory command fast and precise under un-modeled uncertainties and external disturbances. In order to achieve this objective, a recursive integral terminal sliding mode control is developed, which guarantees finite-time convergence of the tracking error to the origin and eliminates the reaching phase commonly present in traditional sliding mode control. The controller design begins by defining the nonsingular terminal sliding function σ_i as follows:

$$\sigma_i = \ddot{e}_i + \lambda_{2i} sig(\dot{e}_i)^{\gamma_{2i}} + \lambda_{1i} sig(e_i)^{\gamma_{1i}}, \quad (8)$$

where the parameters λ_{1i}, λ_{2i} are selected such that the polynomial, which corresponds to the system (6), is Hurwitz. Besides, γ_{1i}, γ_{2i} are selected to satisfy

$$\begin{cases} \gamma_{1i} \in (0,1) \\ \gamma_{2i} = \dfrac{2\gamma_{1i}}{1+\gamma_{1i}} \end{cases} (9)$$

The shorthand notation $sig(x)^y$ originally proposed by Haimo (1986) is a simplified expression given as

$$sig(x)^y = |x|^y sgn(x) (10)$$

where $sgn(x)$ is the signum function. As for all $x \in R$ and $y > 0$, the function $sig(x)^y$ remains smooth and strictly monotonically increasing, and always returns a real-valued output. Importantly, Feng et al. (2014) established that when the sliding function $\sigma_i = 0$ in equation (8), the tracking error e_i converges to the origin in finite-time. A recursive terminal sliding function s_i as follows:

$$s_i = \sigma_i + \lambda_i \sigma_{iI} (11)$$

where σ_i is with (8), $\lambda_i > 0$ and σ_{iI} is designed in the following form:

$$\dot{\sigma}_{iI} = |\sigma_i|^{v_{1i}/v_{2i}} sgn(\sigma_i) (12)$$

where the parameter v_{1i} and v_{2i} are odd positive constants such way are selected $v_{1i} < v_{2i}$ to ensure no singularity occurs. Equation (12) is free of singularities because the term $|\sigma_i|^{v_{1i}/v_{2i}} sgn(\sigma_i)$ remains finite for all σ_i, and evaluates to zero at $\sigma_i = 0$. The condition $v_{1i} < v_{2i}$ ensures that the fractional power exponent lies in (0, 1), avoiding any division by zero. In addition, this property enables finite-time convergence rather than causing a blow-up. To eliminate the reaching phase the initial integral value of σ_{Ii} in (9) is set as

$$\sigma_{Ii}(0) = -\lambda_i^{-1} \sigma_i(0) (13)$$

It can be shown from equations (12) and (13), the initial sliding variable $s_i(0) = 0$, which implies that the control system is enforced to start on the sliding surface at the initial time such that the reaching time is eliminated. Given the initial states of the system are available in most practical settings, $\sigma_{Ii}(0)$ can be determined as follows:

$$\sigma_{Ii}(0) = -\lambda_i^{-1} \left(\ddot{e}_i(0) + \lambda_{2i} sig(\dot{e}_i(0))^{\gamma_2} + \lambda_{1i} sig(e_i(0))^{\gamma_1} \right) (14)$$

When $s_i = 0$ holds in (9), the sliding variable σ_i converges to zero in a finite time t_{si} given by

$$t_{si} = \frac{|\sigma_i(0)|^{\frac{v_{1i}}{v_{2i}}}}{\lambda_i \left(1 - \dfrac{v_{1i}}{v_{2i}} \right)} (15)$$

The final structure of the proposed controller is derived using the recursive integral double terminal sliding function. Its explicit form is given as follows:

$$\tau_i = \tau_{eqi} + \tau_{swi}, (16)$$

where τ_{eqi} and τ_{swi} are the equivalent control input and the reaching control input which will be designed, respectively. By using (3), (8) and (16) and letting $\dot{s}_i = 0$, with $\rho_i = 0$, the following equivalent control input is obtained given as

$$\tau_{eqi}=m_{i0}\left(\ddot{q}_{id}+\lambda_{2i}\,sig\left(\dot{e}_i\right)^{\gamma_{2i}}+\lambda_{1i}\,sig\left(e_i\right)^{\gamma_{1i}}+\lambda_i\,\sigma_{Ii}\right)+c_i\,\dot{q}_i+L_i\,sgn\left(\dot{q}_i\right).\,(17)$$

Moreover, an integral-based control input is designed as

$$\tau_{swi}=m_{i0}\int_0^t\left(\hat{a}_{0i}+\hat{a}_{1i}\left|q_i\right|+\hat{a}_{2i}\left|\dot{q}_i\right|+\hat{a}_{3i}\left|\ddot{q}_i\right|\right)sgn\left(s_i\right)dt\,(18)$$

where the control parameters $\hat{a}_{ji},(j=0,1,2,3)$ are updated using proposed below summation of integral and proportional terms, the following integral adaptive laws given by

$$\dot{\hat{a}}_{0Ii}=\eta_{0Ii}^{-1}\left|s_i\right|\,(19)$$

$$\dot{\hat{a}}_{1Ii}=\eta_{1Ii}^{-1}\left|q_i\right|\left|s_i\right|\,(20)$$

$$\dot{\hat{a}}_{2Ii}=\eta_{2Ii}^{-1}\left|\dot{q}_i\right|\left|s_i\right|\,(21)$$

$$\dot{\hat{a}}_{3Ii}=\eta_{3Ii}^{-1}\left|\ddot{q}_i\right|\left|s_i\right|\,(22)$$

to increase convergence and error suppression, proportional adaptive term with terminal attractor is proposed as

$$\hat{a}_{0pi}=\eta_{0pi}^{-1}\left|s_i\right|^{\beta_i}\,(23)$$

$$\hat{a}_{1pi}=\eta_{1pi}^{-1}\left|q_i\right|\left|s_i\right|^{\beta_i}\,(24)$$

$$\hat{a}_{2pi}=\eta_{2pi}^{-1}\left|\dot{q}_i\right|\left|s_i\right|^{\beta_i}\,(25)$$

$$\hat{a}_{3pi}=\eta_{3pi}^{-1}\left|\ddot{q}_i\right|\left|s_i\right|^{\beta_i}\,(26)$$

and finally

$$\hat{a}_0=\hat{a}_{0p}+\hat{a}_{0I}\,(27)$$

$$\hat{a}_1=\hat{a}_{1p}+\hat{a}_{1I}\,(28)$$

$$\hat{a}_2=\hat{a}_{2p}+\hat{a}_{2I}\,(29)$$

$$\hat{a}_3=\hat{a}_{3p}+\hat{a}_{3I}\,(30)$$

with $\eta_{jpi}>0$, $\eta_{jIi}>0$, $\hat{a}_{jIi}(0)\geq 0$, and $\hat{a}_{jpi}(0)\geq 0$, $(j=0,1,2,3)$. $\beta_i=\dfrac{\beta_{1i}}{\beta_{2i}}$ are positive constants, and β_{1i} and $\beta_{2i}$are two odd positive integers with $\beta_{1i}<\beta_{2i}$. the integral terms gain given in (19 - 22) are used to guarantee convergence of the system to the estimated values, the proportional terms (23 - 26) adds immediate penalty for large errors with terminal attractor and leads the system very quickly toward small tracking errors and reduces the finite-time convergence.

Stability Analysis

The proposed controller stability analysis is provided as follows. From (8) and (9), the derivative of the integral terminal sliding function s_i becomes

$$\dot{s}_i=\dot{\sigma}_i+\lambda_i\,\dot{\sigma}_{Ii},\,(31)$$

the error dynamics are given as

$$\dot{s}_i=\ddot{e}_i+\lambda_{2i}\gamma_{2i}\left|\dot{e}_i\right|^{\gamma_{2i}-1}\ddot{e}_i+\lambda_{1i}\gamma_{1i}\left|e\right|^{\gamma_{2i}-1}\dot{e}_i+\lambda_i\,\dot{\sigma}_{Ii},\,(32)$$

using the dynamics with uncertain in (3) and the proposed τ_{eqi} in (17) the dynamics by integral configuration the following is obtained

$$\dot{s}_i=\frac{d}{dt}\left(\ddot{q}_{id}-m_i^{-1}\left\{\tau_i-c_i\dot{q}_i-L_i\,sgn\left(\dot{q}_i\right)-\rho_i\right\}\right)+\lambda_{2i}\gamma_{2i}\left|\dot{e}_i\right|^{\gamma_{2i}-1}\ddot{e}_i+\lambda_{1i}\gamma_{1i}\left|e\right|^{\gamma_2-1}\dot{e}+\lambda_i\,\dot{\sigma}_{Ii},\,(33)$$

$$\dot{s}_i=-m_i^{-1}\frac{d}{dt}\left(\dot{\tau}_{swi}+\dot{\rho}_i\right),\,(34)$$

Next, the Lyapunov candidate is selected as

$$V_i=\frac{1}{2}s_i^{\,2}+\frac{1}{2}\sum_{i=0}^{3}\mu_{ji}\tilde{a}_{ji}^2,\ (35)$$

where $\mu_{ji}>0$, $\tilde{a}_{ji}=\hat{a}_{ji}-a_{ji}$, $(j=0,1,2,3)$. Solving the derivative of (35) along the system trajectories yields

$$\dot{V}_i=s_i\dot{s}_i+\sum_{j=0}^{3}\mu_{ji}\tilde{a}_{ji}\dot{\tilde{a}}_{ji},\ (36)$$

Using the dynamics of (34) into (36) it becomes

$$\dot{V}_i=-s_i m_i^{-1}\left(\dot{\tau}_{swi}+\dot{\rho}_i\right)+\sum_{j=0}^{3}\mu_{ji}\tilde{a}_{ji}\dot{\tilde{a}}_{ji},\ (37)$$

$$\dot{V}_i=-s_i\left(\left(\hat{a}_{0i}+\hat{a}_{1i}|q_i|+\hat{a}_{2i}|\dot{q}_i|+\hat{a}_{3i}|\ddot{q}_i|\right)sgn(s_i)+\dot{\rho}_i\right)+\sum_{j=0}^{3}\mu_{ji}\tilde{a}_{ji}\dot{\tilde{a}}_{ji},\ (38)$$

Introducing the addition and subtraction of $\left(a_{0i}+a_{1i}|q_i|+a_{2i}|\dot{q}_i|+a_{3i}|\ddot{q}_i|\right)|s_i|$, ??becomes

$$??\leq-\left(\hat{a}_{0i}+\hat{a}_{1i}|q_i|+\hat{a}_{2i}|\dot{q}_i|+\hat{a}_{3i}|\ddot{q}_i|\right)|s_i|+m_i^{-1}|\dot{\rho}_i||s_i|+\sum_{j=0}^{3}\mu_{ji}\tilde{a}_{ji}\dot{\tilde{a}}_{ji}-\left(a_{0i}+a_{1i}|q_i|+a_{2i}|\dot{q}_i|+a_{3i}|\ddot{q}_i|\right)|s_i|$$

$$+\left(a_{0i}+a_{1i}|q_i|+a_{2i}|\dot{q}_i|+a_{3i}|\ddot{q}_i|\right)|s_i|,\ (39)$$

$\tilde{a}_{ji}=\hat{a}_{jIi}-a_{ji}$ and $\dot{\tilde{a}}_{ji}=\dot{\hat{a}}_{jIi}$, $(j=0,1,2,3)$ further more $\hat{a}_{ji}=\hat{a}_{jpi}+\hat{a}_{jIi}$ and

$$\leq-\left(\hat{a}_{0i}+\hat{a}_{1i}|q_i|+\hat{a}_{2i}|\dot{q}_i|+\hat{a}_{3i}|\ddot{q}_i|\right)|s_i|+m_i^{-1}|\dot{\rho}_i||s_i|+\mu_{0i}\tilde{a}_{0i}\dot{\hat{a}}_{0Ii}+\mu_{1i}\tilde{a}_{1i}\dot{\hat{a}}_{1Ii}+\mu_{2i}\tilde{a}_{2i}\eta_{2Ii}^{-1}|\dot{q}_i||s_i|+\mu_{3i}\tilde{a}_{3i}\dot{\hat{a}}_{3Ii}-\left(a_{0i}+a_{1i}|q_i|+a_{2i}|\dot{q}_i|+a_{3i}|\ddot{q}_i|\right)|s_i|$$

$$\leq-\left(\left(\hat{a}_{0pi}+\hat{a}_{0Ii}\right)+\left(\hat{a}_{1pi}+\hat{a}_{1Ii}\right)|q_i|+\left(\hat{a}_{2pi}+\hat{a}_{2Ii}\right)|\dot{q}_i|+\left(\hat{a}_{3pi}+\hat{a}_{3Ii}\right)|\ddot{q}_i|\right)|s_i|+m_i^{-1}|\dot{\rho}_i||s_i|+\mu_{0i}\tilde{a}_{0i}\dot{\hat{a}}_{0Ii}+\mu_{1i}\tilde{a}_{1i}\dot{\hat{a}}_{1Ii}+\mu_{2i}\tilde{a}_{2i}\eta_{2Ii}^{-1}|\dot{q}_i||s_i|+\mu_{3i}\tilde{a}_{3i}\dot{\hat{a}}_{3Ii}-\left(a_{0i}+a_{1i}|q_i|+a_{2i}|\dot{q}_i|+a_{3i}|\ddot{q}_i|\right)|s_i|$$

$$+\left(a_{0i}+a_{1i}|q_i|+a_{2i}|\dot{q}_i|+a_{3i}|\ddot{q}_i|\right)|s_i|,\ (40)$$

$$+\left(a_{0i}+a_{1i}|q_i|+a_{2i}|\dot{q}_i|+a_{3i}|\ddot{q}_i|\right)|s_i|.\ (41)$$

Now apply this equations (19) – (22) it becomes

$$??\leq-\left(\hat{a}_{0pi}+\hat{a}_{1pi}|q_i|+\hat{a}_{2pi}|\dot{q}_i|+\hat{a}_{3pi}|\ddot{q}_i|\right)|s_i|-\left(\tilde{a}_{0i}+\tilde{a}_{1i}|q_i|+\tilde{a}_{2i}|\dot{q}_i|+\tilde{a}_{3i}|\ddot{q}_i|\right)|s_i|$$

$$+m_i^{-1}|\dot{\rho}_i||s_i|+\mu_{0i}\tilde{a}_{0i}\eta_{0Ii}^{-1}|s_i|+\mu_{1i}\tilde{a}_{1i}\eta_{1Ii}^{-1}|q_i||s_i|+\mu_{2i}\tilde{a}_{2i}\eta_{2Ii}^{-1}|\dot{q}_i||s_i|+\mu_{3i}\tilde{a}_{3i}\eta_{3Ii}^{-1}|\ddot{q}_i||s_i|-\left(a_{0i}+a_{1i}|q_i|+a_{2i}|\dot{q}_i|+a_{3i}|\ddot{q}_i|\right)|s_i|,\ (42)$$

Suppose $\hat{a}_{0Ii}\leq a_i$ and substituting equations (23) – (26)

$$\leq-\left(\eta_{0pi}^{-1}+\eta_{1pi}^{-1}|q_i|^2+\eta_{2pi}^{-1}|\dot{q}_i|^2+\eta_{3pi}^{-1}|\ddot{q}_i|^2\right)|s_i|^{\beta_i+1}$$

$$-\left(\mu_{0i}\eta_{0Ii}^{-1}-1\right)|\tilde{a}_{0i}||s_i|-\left(\mu_{1i}\eta_{1Ii}^{-1}-1\right)|q_i||\tilde{a}_{1i}||s_i|$$

$$-\left(\mu_{2i}\eta_{2Ii}^{-1}-1\right)|\dot{q}_i||\tilde{a}_{2i}||s_i|-\left(\mu_{3i}\eta_{3Ii}^{-1}-1\right)|\ddot{q}_i||\tilde{a}_{3i}||s_i|$$

$$-\left(a_{0i}+a_{1i}|q_i|+a_{2i}|\dot{q}_i|+a_{3i}|\ddot{q}_i|-m_i^{-1}|\dot{\rho}_i|\right)|s_i|,\ (43)$$

by defining the following symbols

$$\sigma_{si}=a_{0i}+a_{1i}|q_i|+a_{2i}|\dot{q}_i|+a_{3i}|\ddot{q}_i|-m_i^{-1}|\dot{\rho}_i|,\ (44)$$

$$\sigma_{ji}=\left(\mu_{ji}\eta_{jIi}^{-1}-1\right)\left|q_i^{(j)}\right||s_i|,\ (45)$$

$$\sigma_{pi}=\eta_{0pi}^{-1}+\eta_{1pi}^{-1}|q_i|^2+\eta_{2pi}^{-1}|\dot{q}_i|^2+\eta_{3pi}^{-1}|\ddot{q}_i|^2,\ (46)$$

where $i=0,1,2,3$. Then, if $\sigma_{si},\sigma_{ji},\sigma_{pi}>0$, (43) can be rewritten as

$$\dot{V}\le-\sigma_{si}|s_i|-\sum_{j=0}^{3}\sigma_{ji}|\tilde{a}_{ji}|-\sigma_{pi}|s_i|^{\beta_i+1} \quad (47)$$

$$\le-\sigma_{si}\sqrt{2}\frac{|s_i|}{\sqrt{2}}-\sum_{j=0}^{3}\sigma_{ji}\sqrt{\frac{2}{\mu_{ji}}}\sqrt{\frac{\mu_{ji}}{2}}|\tilde{a}_{ji}|-\sigma_{pi}|s_i|^{\beta_i+1} \quad (48)$$

$$\le-\left(\frac{|s_i|}{\sqrt{2}}+\sum_{j=0}^{3}\sigma_{ji}\sqrt{\frac{\mu_{ji}}{2}}|\tilde{a}_{ji}|\right)min\left\{\sigma_{si}\sqrt{2},\sigma_{ji}\sqrt{\frac{2}{\mu_{ji}}}\right\}-\sigma_{pi}|s_i|^{\beta_i+1} \quad (49)$$

$$\le-\Gamma_{1i}V_i^{1/2}-\Gamma_{2i}V_i^{(\beta_i+1)/2} \quad (50)$$

where Γ_{1i}, Γ_{2i} are positive constants satisfying:

$$\Gamma_{1i}\le min\left\{\sigma_{si}\sqrt{2},\sigma_{ji}\sqrt{\frac{2}{\mu_{ji}}}\right\},\Gamma_{2i}=\sigma_{pi}2^{(\beta_i+1)/2}, \quad (51)$$

It is evident that $\sigma_{si}>0$, and for any values $\eta_{jpi}^{-1},\eta_{jIi}^{-1},(j=0,1,2,3)$, there exists suitable constants μ_{ji},a_{ji} such that $\sigma_{ji}>0$, and $\Gamma_{1i},\Gamma_{2i}>0$. For that instance, the inequality (50) satisfies the finite-time stability condition. More specifically, V will converge to zero in finite-time from condition $V_i(0)$, and the convergence of the time satisfies

$$t_{vi}\le\frac{2V_i^{1/2}(0)}{\Gamma_{1i}}+\frac{2V_i^{(1-\beta_i)/2}(0)}{(\beta_i-1)\Gamma_{2i}}. \quad (52)$$

It follows that the sliding variable s_i and the estimation error $\tilde{a}_i$ will both diminish to zero in finite time. Once s_i becomes zero, the quantities σ_i and e_i will sequentially converge to zero over their respective finite intervals t_{si} and $t_{\sigma i}$. Consequently, the tracking error e_i will vanish in a finite time $t_{ci}=t_{vi}+t_{si}+t_{\sigma i}$, regardless of the initial condition. This completes the proof.

Selecting Control Parameters

When implementing the controller, it's necessary to balance the trade-offs between signal smoothness, power consumption, and measurement noise. The control parameters selection guideline for the proposed controller is as follows.

1) Values of λ_{1i}, λ_{2i}, γ_{1i} and γ_{2i} in the terminal sliding surface enhance the convergence rate of the tracking error e_i to zero, so are selected large. However, large values result in a larger control input, which can increase chattering and energy consumption. Ultimately, the selection of these parameters should consider system dynamics and actuator limitations.
2) The parameter $\lambda_1,\lambda_2>0$ is chosen to balance the rate of convergence and the magnitude of the control input; larger values improve convergence but may increase control effort and chattering. The exponents v_{1i} and v_{2i} are selected as odd positive integers such that $v_{2i}<v_{1i}$, which ensures finite-time convergence of the integral term while avoiding singularity at $\sigma_i=0$.
3) Choosing small values for η_{jpi} , η_{jIi}, $(j=1,2,3,4)$ enables faster estimation of the control gain, as shown in (19) – (26). However, it may cause overestimation or even lead to control input saturation of the servo drive.

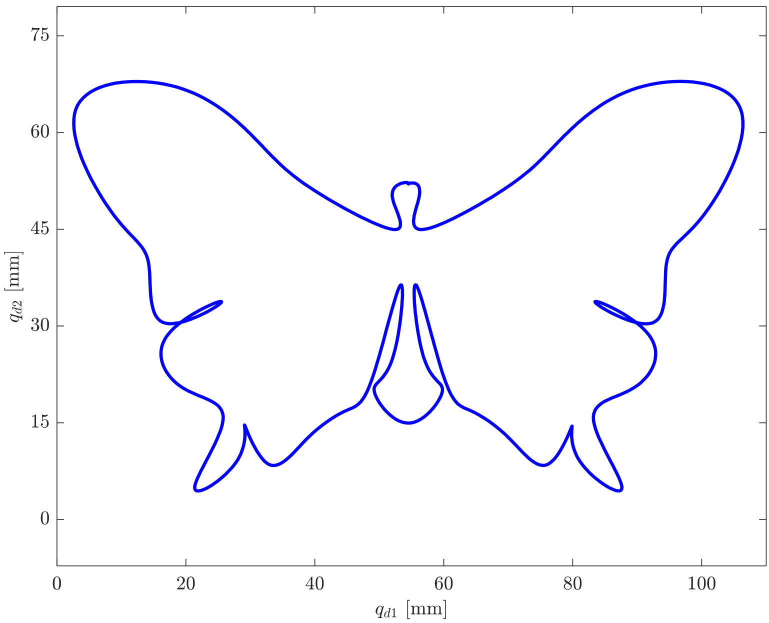

Figure 1: Butterfly reference trajectory

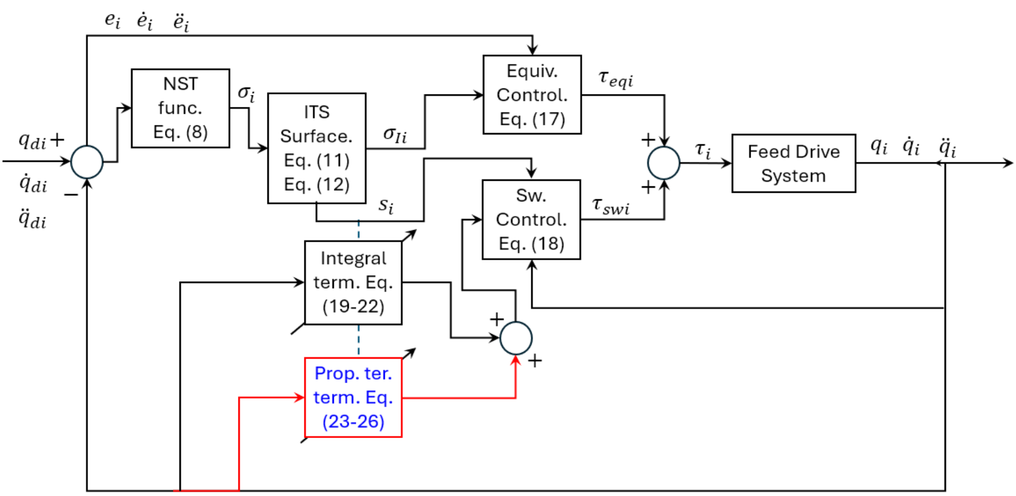

Figure 2: Proposed approach schematic

Simulation

To validate the effectiveness of the proposed method as shown in Figure 2, simulation is conducted based on Butterfly reference trajectories in Figure 1 for both axes. From Figure 2 upon removing the red block it becomes the conventional approach of SO-RTSM from Deng et al. (2020). The butterfly trajectory poses challenges because of its sharp curvatures and frequent changes in direction, which demand high controller precision with fast dynamic response. In addition, its abrupt segments make it more difficult to track accurately compared to standard test paths like circles or lemniscates. The nonlinear second order plant in (3) is considered as the real system. External disturbances fused with the states given as $\rho_i = 300 + 100 q_i + 100 \dot{q}_i + 100 \ddot{q}_i N$ for both axes are applied to evaluate the performance in presence of matched uncertainty. The other plant and controller parameters are given in Tables 2 and 3 respectively. Only by $\hat{a}_{0I}, \hat{a}_{1I}, \hat{a}_{2I}$, and $\hat{a}_{3I}$ in Table 3 is a used for the controller design from Deng et al. (2020) also defined as SO-RTSM and for the proposed $\hat{a}_{0I}, \hat{a}_{1I}, \hat{a}_{2I}$, and $\hat{a}_{3I}$ are added with proportional terminal gains $\hat{a}_{0p}, \hat{a}_{1p}, \hat{a}_{2p}$, and $\hat{a}_{3p}$ to increase disturbance suppression.

Table 2: Dynamic parameters

i^{th} **axis**	$m_{0i}[N s^2/m]$	$c_{0i}[Ns/m]$	$L_{0i}[N]$	$K_{\mu i}[N/A]$	$Z_i[\Omega]$
1	88.08	467.20	45.50	124.76	10.00
2	97.90	631.00	54.80	200.22	15.00

Table 3: Control Parameters

Control Parameter	1^{st} **axis**	2^{nd} **axis**
$\lambda_{1i}, \lambda_{2i}$	$80e4, 1e3$	$80e4, 1e3$
γ_{1i}	0.9	0.9
λ_i	$80e2$	$80e2$
$\eta_{0Ii}^{-1}, \eta_{1Ii}^{-1}, \eta_{2Ii}^{-1}, \eta_{3Ii}^{-1}$	$10, 0.01, 0.001, 0.0001$	$10, 0.01, 0.001, 0.0001$
$\eta_{0pi}^{-1}, \eta_{1pi}^{-1}, \eta_{2pi}^{-1}, \eta_{3pi}^{-1}$	$60, 0.06, 0.006, 0.0006$	$60, 0.06, 0.006, 0.0006$
β_i	$99/101$	$99/101$

Figure 3 shows the absolute contour error distribution from Cheng and Lee (2007), a butterfly trajectory tracking task using two different control strategies: (a) SO-RTSM proposed by Deng et al. (2020) and (b) the Proposed method. Both subplots visualize the error contour magnitude across the trajectory path in 3D, with the color map code indicating the error scale from 0 to 2.5×10^{-3}mm. As seen in Figure 3 (a), the SO-RTSM method shows relatively higher error contour magnitudes, particularly in areas with high curvature or rapid directional changes. The red and orange areas in the Figure 3 indicate that the error frequently exceeds 1.5×10^{-3}mm, suggesting limitations in the adaptability of this controller. In contrast, Figure 3 (b), demonstrates a significant improvement using the proposed control approach as compared to SO-RTSM. The contour error is consistently lower, with most of the path maintaining values under 0.5×10^{-3} mm as indicated by the dominance of green in the color spectrum. Only minor regions exhibit slight increases in error, but these remain well below the peak values observed in the SO-RTSM case.

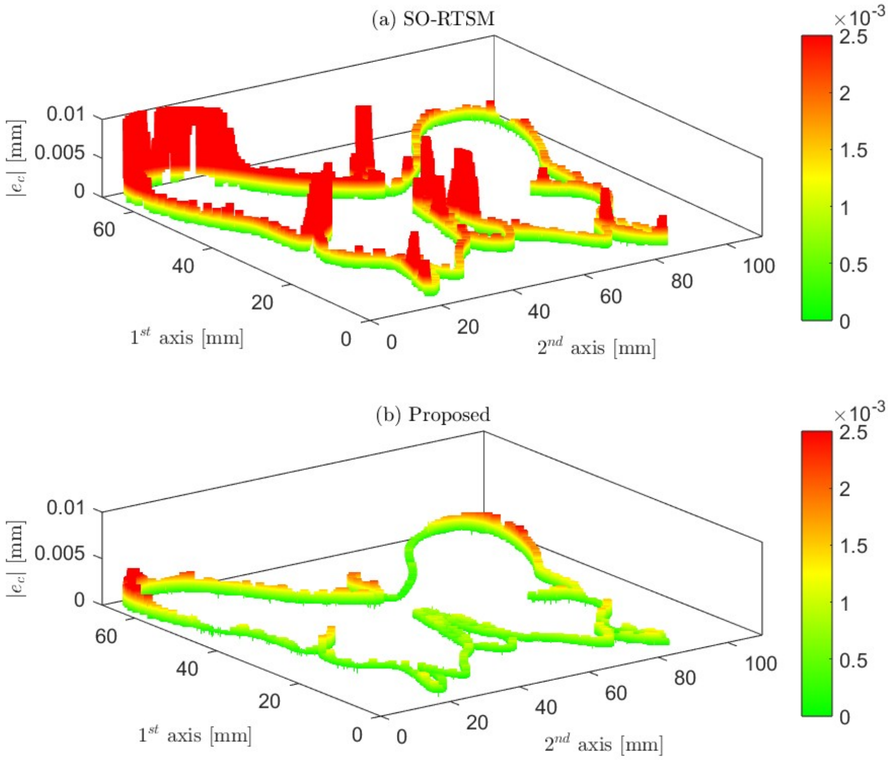

Figure 3: 3D Overall tracking performance

Figure 4 shows a detailed comparison of the SO-RTSM and Proposed control over a 10-second period for both the first and second motion axes of the butterfly trajectory. The first and second row of plots shows that both approaches achieve accurate tracking across the entire time span, without noticeable deviation. In the third row, the absolute tracking errors $|q_i - q_{di}|$ for both axes confirms the superior precision of the Proposed method, maintaining lower tracking errors mostly below 1.5×10^{-3} mm throughout the 10s duration, while the SO-RTSM shows spikes fluctuations reaching over 5×10^{-3}mm, particularly towards the final seconds of the simulation. Finally, the fourth row indicates cumulative energy consumption over time, the energy consumption is described and adopted from Nshama et al. (2021): for the first axis, SO-RTSM energy use rises steadily from 350 J to over 400 J, while the Proposed method levels off around 375 J; for the second axis, the energy savings are even more pronounced, with the Proposed method consuming approximately 30 J less by the end of the 10 s period. These results highlight the Proposed controller’s advantage in achieving more accurate tracking with smoother control signals and reduced energy demands across the full duration of the task under uncertainty and external disturbances.

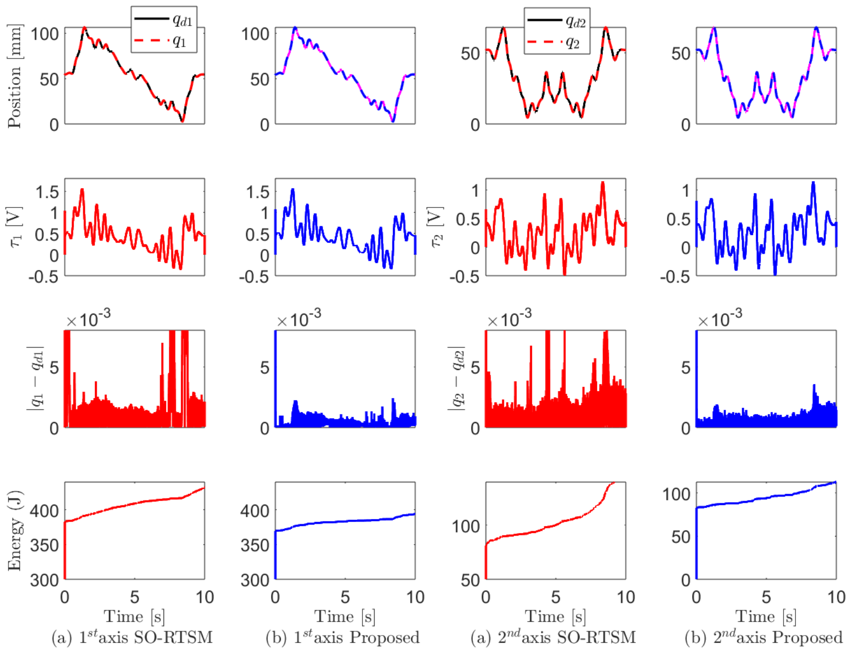

Figure 4: Individual axis tracking and control input performance

Figure 5 shows adaptive gains used to compensate for disturbances over a 10-second duration, comparing the SO-RTSM and Proposed control strategies for both motion axes. It is evident that the integral gains in the Proposed method remain consistently lower than those in the SO-RTSM approach across all components. This difference can be attributed to the improved tracking accuracy and disturbance rejection capability of the Proposed controller, which requires less aggressive adaptation to maintain performance. In SO-RTSM, the larger tracking errors and less stable control inputs as shown in Figure 4 third row, result in more pronounced disturbance effects, causing the adaptive law to respond with significantly higher gain values, where several gain terms rapidly increase. In contrast, the Proposed method achieves better initial tracking and disturbance mitigation, leading to slower and smoother gain. This behavior not only reflects greater energy-saving but also indicates that the Proposed method relies less on compensatory adaptation, emphasizing its superior.

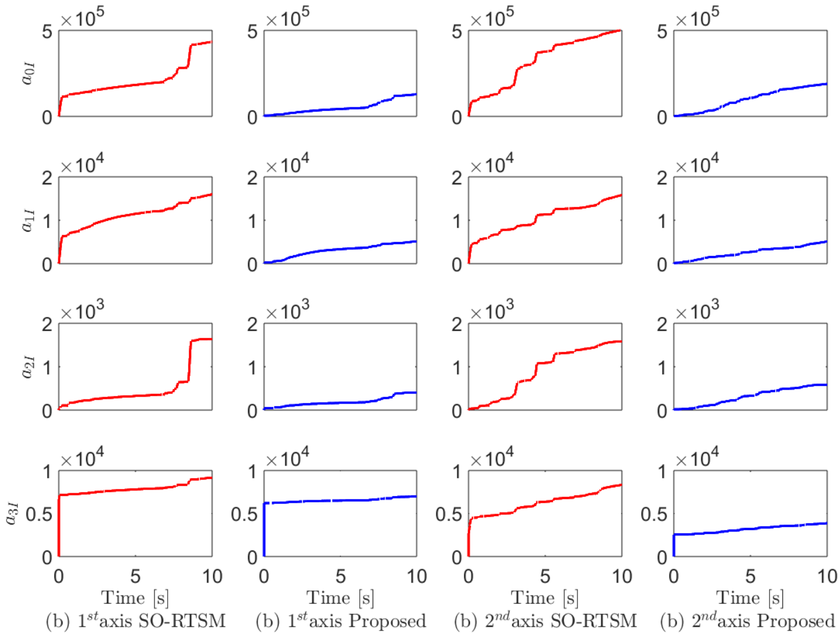

Figure 5: Adaptive integral gains

The proposed controller introduces an additional set of adaptive proportional terminal gains**,** which are incorporated alongside the existing integral gains, these gains are shown in Figure 6. This modification represents the only difference from the earlier version of SO-RTSM. The proportional terminal gain follows a power-law formulation, similar to that used in terminal sliding mode control architecture, enabling rapid convergence by amplifying the corrective action when the tracking error is large, and gradually reducing it as the system nears the target. This nonlinear gain behavior significantly enhances the transient response; the controller reacts more aggressively to deviations. Proposed method with proportional terminal gain achieves superior performance using less overall adaptation effort, benefiting from the fast finite-time convergence properties characteristic of proportional terminal term while maintaining smooth, energy-saving. The finite-time convergence is shown in the Figure 7 for which its described in the log scale in the 1 second of the whole trajectory, comparing SO-RTSM and the proposed method. The proposed method achieves finite-time convergence at around 0.077 seconds, stabilizing to a lower contour error magnitude more quickly and consistently than SO-RTSM, which converges at around 0.363 seconds**.** Table 4 compares the SO-RTSM and the proposed approach in terms of tracking error, energy consumption, and convergence time for 2 axes of the feed drive following butterfly trajectory. The proposed method outperforms SO-RTSM by achieving significantly lower tracking errors, reduced energy consumption, and much faster convergence to steady-state.

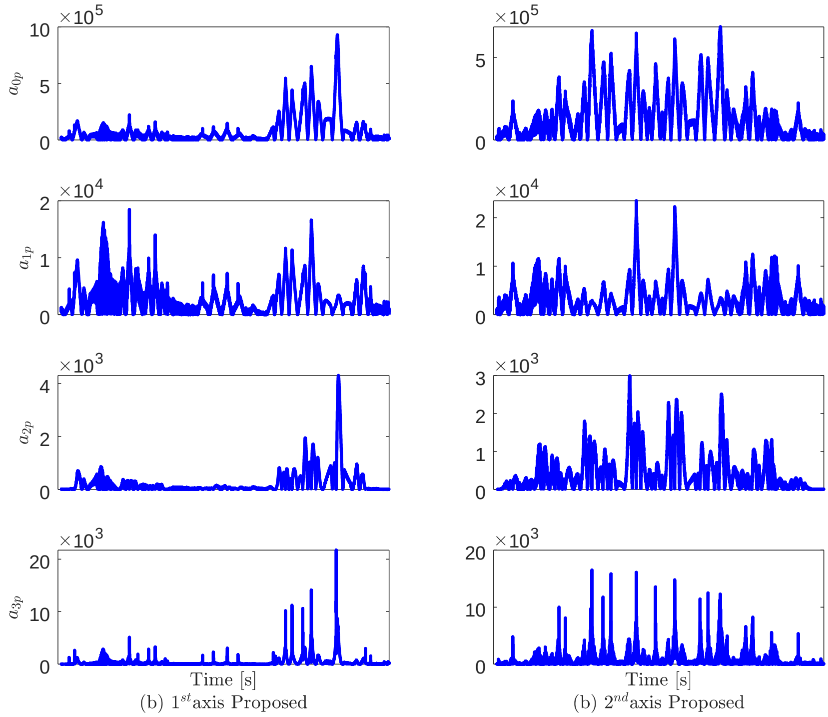

Figure 6: Proportional terminal gain

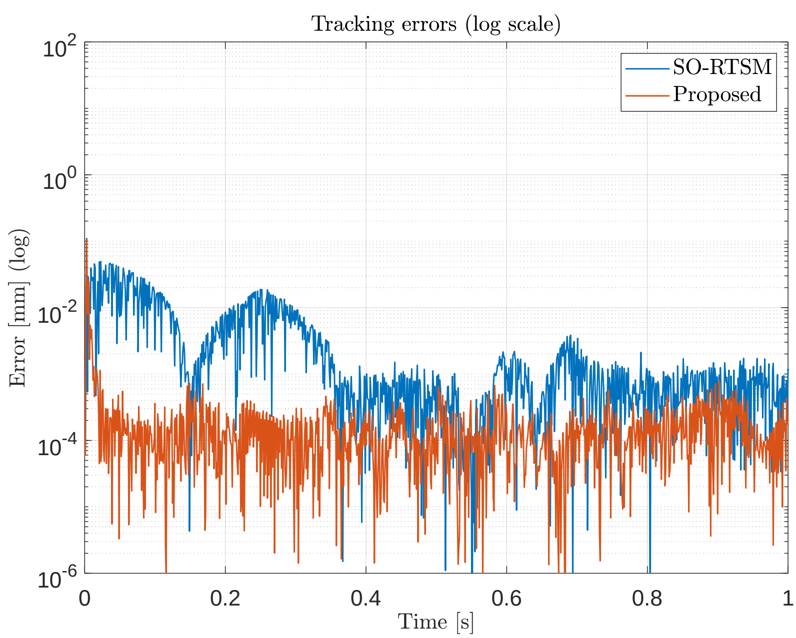

Figure 7: Finite-time convergence

Table 4: Summary of the results as comparison between SO-RTSM and proposed approach

	Absolute average tracking error [mm]		Average Energy Consumption [J]		Time convergence to steady state error [s]	
Approaches	1st axis	2nd axis	1st axis	2nd axis	1st axis	2nd axis
SO-RTSM	0.002351	0.001226	406.86	105.48	0.329	0.022
Proposed	0.000412	0.000478	382.66	95.28	0.010	0.008

Discussion

The superior performance of the proposed controller over the SO-RTSM can be attributed to several key design enhancements. The inclusion of the proportional terminal adaptive gains on the equations (23)-(26) enables continuous compensation for persistent disturbances, resulting in significantly reduced steady-state tracking errors. Second, the proportional terminal gains introduce nonlinear terminal error feedback with a power factor that amplifies the transient performance by accelerating convergence during large initial errors. Unlike SO-RTSM, which relies on high gain magnitudes to correct deviations, the proposed method achieves similar or better accuracy with smoother and more efficient control signals, reducing energy consumption. The term $\left|s_i\right|^{\beta_i}$ in the equations (23)-(26), possess a non-linear behaviour, such that the function grows more slowly when s_i is large and becomes more sharply when s_i is small. This means that in the transient phase, the control effort is relatively mild, resulting in moderate energy used compared to the case with $\beta_i = 1$. However, in the steady-state region, where s_i becomes small, the term $\left|s_i\right|^{\beta_i}$ it becomes relatively large near the origin, which causes the controller to continue applying aggressive control effort even when the error is small. This ensures adaptation and errors become smaller. Moreover, the obtained results are consistent with recent studies on adaptive control approaches summarized in Zhang et al. (2021) as well as Harada and Uchiyama (2021), which similarly reported enhanced convergence rates and energy efficiency under addition of proportional term in feedback.

As future works, it is interesting to consider including fast terminal proportional and integral terms in the compensation of the uncertainties and external disturbances and consider improving contouring performance. In addition, Figure 8 describes control inputs from both methods, with only small deviations visible at certain peaks and transitions at 0-0.5, 3-4.5 and 8.5-10 seconds. The Proposed approach achieves smoother compared to the SO-RTSM. Overall, the Proposed approach appears slightly less aggressive in high-frequency fluctuations.

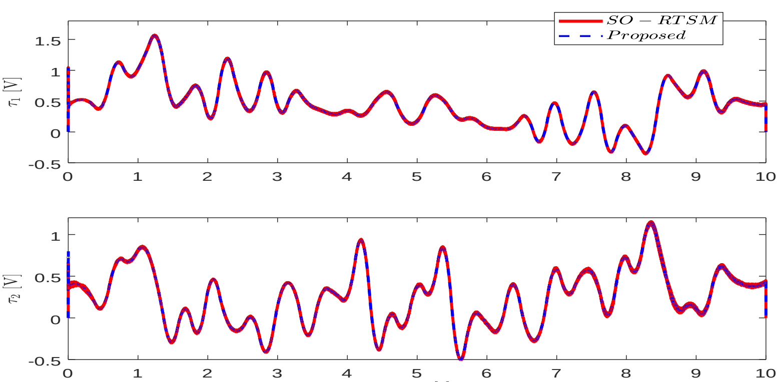

Figure 8: Control input comparison

Conclusion

This study presents a novel adaptive control framework for precision trajectory tracking in biaxial feed drive systems, integrating nonlinear adaptive proportional-integral gains with recursive terminal sliding mode-inspired dynamics. The proposed controller leverages fractional power-based adaptation law on the proportional term, enabling faster convergence during transients and minimal control effort near steady-state, which contributes to overall energy-saving. Furthermore, finite-time is guaranteed. Numerical simulation results demonstrated that the controller consistently achieves sub-micron tracking accuracy, with smoother control signals and up to 30 J energy savings per axis over a 10-second butterfly trajectory. The introduction of proportional terminal gains significantly enhances transient performance without compromising steady-state accuracy, while maintaining stable gain evolution. Overall, the proposed control architecture achieves a superior balance between speed, precision, and energy-saving, making it well-suited for high-performance industrial motion systems requiring both accuracy and sustainable operation.

Declaration of Interest

The author declares that there is no conflict of interest concerning this work.

REFERENCES

Altintas Y, Verl A, Brecher C, Uriarte L and Pritschow G 2011. Machine tool feed drives. *CIRP Ann.*, 60(2): 779–796. https://doi.org/10.1016/j.cirp.2011.05.010.

Boiko IM 2013. Chattering in sliding mode control systems with boundary layer approximation of discontinuous control. *Int. J. Syst. Sci.*, 44(6): 1126–1133. https://doi.org/10.1080/00207721.2011.652233.

Chen L, Zhang H, Wang H, Shao K, Wang G and Yazdani A 2023. Continuous adaptive fast terminal sliding mode-based speed regulation control of PMSM drive via improved super-twisting observer. *IEEE Trans. Ind. Electron.*, 71(5): 5105–5115. https://doi.org/10.1109/TIE.2023.3288147.

Cheng MY and Lee CC 2007. Motion controller design for contour-following tasks based on real-time contour error estimation. *IEEE Trans. Ind. Electron.*, 54(3): 1686–1695. https://doi.org/10.1109/TIE.2007.894691.

Chiu CS 2012. Derivative and integral terminal sliding mode control for a class of MIMO nonlinear systems. *Automatica*, 48(2): 316–326. https://doi.org/10.1016/j.automatica.2011.08.055.

Deng B, Shao K and Zhao H 2020. Adaptive second-order recursive terminal sliding mode control for a four-wheel independent steer-by-wire system. *IEEE Access*, 8: 75936–75945. https://doi.org/10.1109/ACCESS.2020.2989326.

Dong RQ, Wu AG, Zhang Y and Duan GR 2021. Anti-unwinding sliding mode attitude control via two modified Rodrigues parameter sets for spacecraft. *Automatica*, 129: 109642. https://doi.org/10.1016/j.automatica.2021.109642.

Feng Y, Yu X and Man Z 2002. Non-singular terminal sliding mode control of rigid manipulators. *Automatica*, 38(12): 2159–2167. https://doi.org/10.1016/S0005-1098(02)00147-4.

Feng Y, Han F and Yu X 2014. Chattering-free full-order sliding mode control. *Automatica*, 50(4): 1310–1314. https://doi.org/10.1016/j.automatica.2014.01.004.

Gai H, Li X, Jiao F, Cheng X, Yang X and Zheng G 2021. Application of a new model reference adaptive control based on PID control in CNC machine tools. *Machines*, 9(11): 274. https://doi.org/10.3390/machines9110274.

Gambhire SJ, Kishore DR, Londhe PS and Pawar SN 2021. Review of sliding mode based control techniques for control system applications. *Int. J. Dyn. Control*, 9(1): 363–

378. https://doi.org/10.1007/s40435-020-00638-7.

Haimo VT 1986. Finite time controllers. *SIAM J. Control Optim.*, 24(4): 760–770. https://doi.org/10.1137/0324047.

Halinga MS, Nyobuya HJ and Uchiyama N 2023. Energy-optimal coverage motion trajectory generation for industrial machines. *IFAC-Pap. Online*, 56(2): 8758–8763. https://doi.org/10.1016/j.ifacol.2023.10.060.

Harada S and Uchiyama N 2021. Robust simple adaptive control with augmented output signal and friction compensation for industrial feed drive systems. *Proc. IEEE Int. Conf. Ind. Technol.* 1: 99–104. https://doi.org/10.1109/ICIT46573.2021.9453499

Kaufman H, Barkana I and Sobel K 2012. *Direct Adaptive Control Algorithms: Theory and Applications.* Springer, Berlin.

Leipe V, Hinze C, Lechler A and Verl A 2023. Model predictive control for compliant feed drives with offset-free tracking behavior. *Prod. Eng.*, 17(6): 805–814. https://doi.org/10.1007/s11740-023-01206-6.

Msukwa M and Santos K 2021. Adaptive sliding mode contouring control design based on reference adjustment and uncertainty compensation for feed drive systems. *Tanzan. J. Sci.*, 47(5): 1766–1778. https://doi.org/10.4314/tjs.v47i5.23.

Msukwa MR, Nshama EW and Uchiyama N 2020. Adaptive sliding mode control with feedforward compensator for energy-efficient and high-speed precision motion of feed drive systems. *IEEE Access*, 8: 43571–43581. https://doi.org/10.1109/ACCESS.2020.2977395.

Nshama EW, Msukwa MR and Uchiyama N 2021. A trade-off between energy saving and cycle time reduction by Pareto optimal corner smoothing in industrial feed drive systems. *IEEE Access*, 9: 23579–23594. https://doi.org/10.1109/ACCESS.2021.3056755.

Nyobuya HJ and Uchiyama N 2024. Combined simple adaptive and integral terminal sliding mode control for industrial feed drive systems. *Control Eng. Pract.*, 153: 106109. https://doi.org/10.1016/j.conengprac.2024.106109.

Oliveira TR, Hsu L and Nunes EVL 2022. Smooth sliding control to overcome chattering arising in classical SMC and super-twisting algorithm in the presence of unmodeled dynamics. *J. Frankl. Inst.*, 359(2): 1235–1256. https://doi.org/10.1016/j.jfranklin.2021.11.005.

Önen Ü 2023. Model-free controller design for nonlinear under-actuated systems with uncertainties and disturbances by using extended state observer based chattering-free sliding mode control. *IEEE Access*, 11: 2875–2885. https://doi.org/10.1109/ACCESS.2023.3234864.

Razzaghian A, Kardehi MR and Pariz N 2022. Adaptive fuzzy fractional-order fast terminal sliding mode control for a class of uncertain nonlinear systems. *Int. J. Ind. Electron. Control Optim.*, 5(1): 77–87.

Saha S, Amrr SM, Saidi AS, Banerjee A and Nabi M 2021. Finite-time adaptive higher-order SMC for the nonlinear five DOF active magnetic bearing system. *Electronics*, 10(11): 1333. https://doi.org/10.3390/electronics10111333.

Shtessel Y, Plestan F, Edwards C and Levant A 2023. Adaptive sliding mode and higher-order sliding mode control techniques with applications: a survey. In: *Sliding-Mode Control and Variable-Structure Systems: The State of the Art*, pp. 267–305. Springer, Cham. https://doi.org/10.1007/978-3-031-37089-2_11.

Slotine JJE and Li W 1991. *Applied Nonlinear Control.* Prentice Hall, Englewood Cliffs, NJ.

Sun Y, Yang M, Wang B, Chen Y and Xu D 2022. Precise position control based on resonant controller and second-order sliding mode observer for PMSM-driven feed servo system. *IEEE Trans. Transp. Electrific.*, 9(1): 196–209. https://doi.org/10.1109/TTE.2022.3182027.

Utkin V 2015. Discussion aspects of high-order sliding mode control. *IEEE Trans. Autom. Control.*, 61(3): 829–833. https://doi.org/10.1109/TAC.2015.2450571.

Vo AT and Kang HJ 2019. A chattering-free, adaptive, robust tracking control scheme for nonlinear systems with uncertain dynamics. *IEEE Access*, 7: 10457–10466. https://doi.org/10.1109/ACCESS.2019.2891763.

Wei Y, Zhang S, Chen Y and Karimi HR 2025. Dynamic sliding mode control for ball screw drive systems under a disturbance observer scheme. *J. Frankl. Inst.*, 362(4): 107517. https://doi.org/10.1016/j.jfranklin.2025.107517.

Wu Y, Yu X and Man Z 1998. Terminal sliding mode control design for uncertain dynamic systems. *Syst. Control Lett.*, 34(5): 281–287. https://doi.org/10.1016/S0167-6911(98)00036-X.

Xu H, Hinze C, Iannelli A and Verl A 2024. Robust inversion-based feedforward control with hybrid modeling for feed drives. *IEEE Trans. Control Syst. Technol.*, https://doi.org/10.1109/TCST.2024.3512862.

Yu S, Yu X, Shirinzadeh B and Man Z 2005. Continuous finite-time control for robotic manipulators with terminal sliding mode. *Automatica*, 41(11): 1957–1964. https://doi.org/10.1016/j.automatica.2005.07.001.

Yu Z, Liu N, Wang K, Sun X and Sheng X 2023. Design of fuzzy PID controller based on sparse fuzzy rule base for CNC machine tools. *Machines*, 11(1): 81. https://doi.org/10.3390/machines11010081.

Zamfirache IA, Precup RE, Roman RC and Petriu EM 2023. Neural network-based control using actor–critic reinforcement learning and grey wolf optimizer with experimental servo system validation. *Expert Syst. Appl.*, 225: 120112. https://doi.org/10.1016/j.eswa.2023.120112.

Zhang C, Pei S and Mohammadzadeh A 2025. An adaptive-switching fuzzy structural vibration control system: theory and experiment. *J. Vib. Eng. Technol.*, 13(5): 1–25. https://doi.org/10.1007/s42417-025-01881-y.

Zhang Z, Yang Z, Xiong S, Chen S, Liu S and Zhang X 2021. Simple adaptive control-based reconfiguration design of cabin pressure control system. *Complexity*, 2021(1): 6635571. https://doi.org/10.1155/2021/6635571

Zhong G, Wang C and Dou W 2021. Fuzzy adaptive PID fast terminal sliding mode controller for a redundant manipulator. *Mech. Syst. Signal Process.*, 159: 107577. https://doi.org/10.1016/j.ymssp.2020.107577.

Zuo Y, Lai C and Iyer KLV 2023. A review of sliding mode observer-based sensorless control methods for PMSM drive. *IEEE Trans. Power Electron.*, 38(9): 11352–11367. https://doi.org/10.1109/TPEL.2023.3287828